

# Colloid transport in water saturated porous media: dispersivity, cotransport and gravity effects

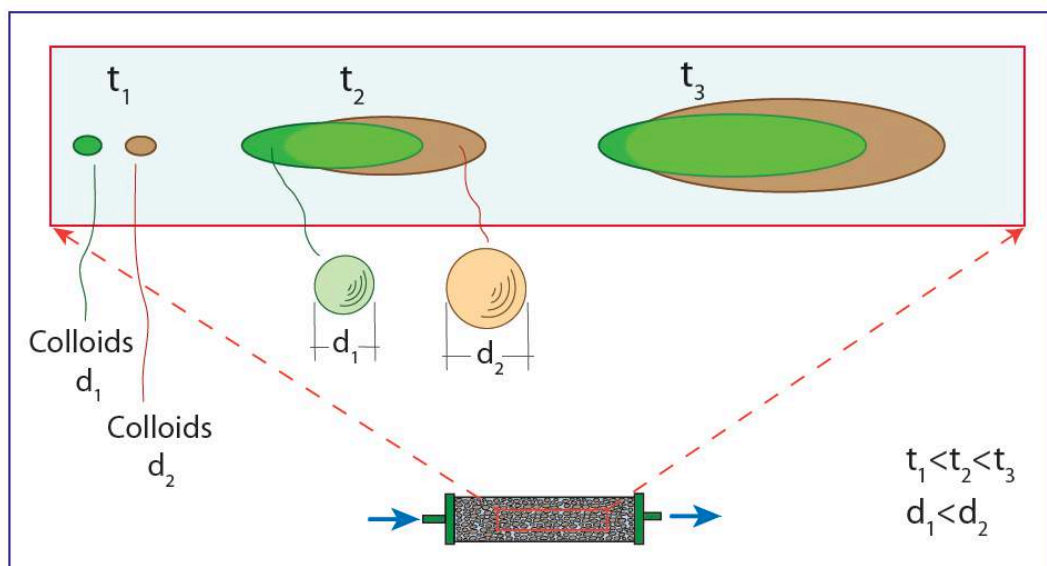
Constantinos V. Chrysikopoulos<sup>1</sup>, Vasileios E. Katzourakis<sup>2</sup>  
and Vasiliki I. Syngouna<sup>2</sup>

<sup>1</sup>School of Environmental Engineering, Technical University of Crete, Greece.

<sup>2</sup>Department of Civil Engineering, University of Patras, Greece



## Part A: Colloid Size-dependent dispersivity



# Previous studies

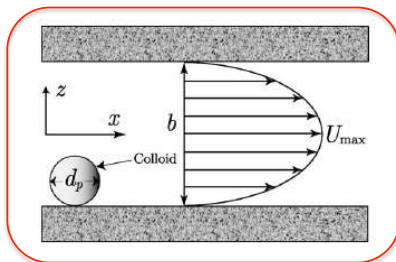
Early breakthrough of colloids as compared to conservative tracers

“Larger colloids are restricted by the size exclusion effect from sampling all paths”

## References:

Toran and Palumbo, 1992  
 Powelson et al., 1993  
 Grindrod et al., 1996  
 Dong et al., 2002  
 Keller et al., 2004.  
 Vasiliadou and Chrysikopoulos, 2011  
 Sinton et al., 2012

## Effective dispersion in a uniform fracture

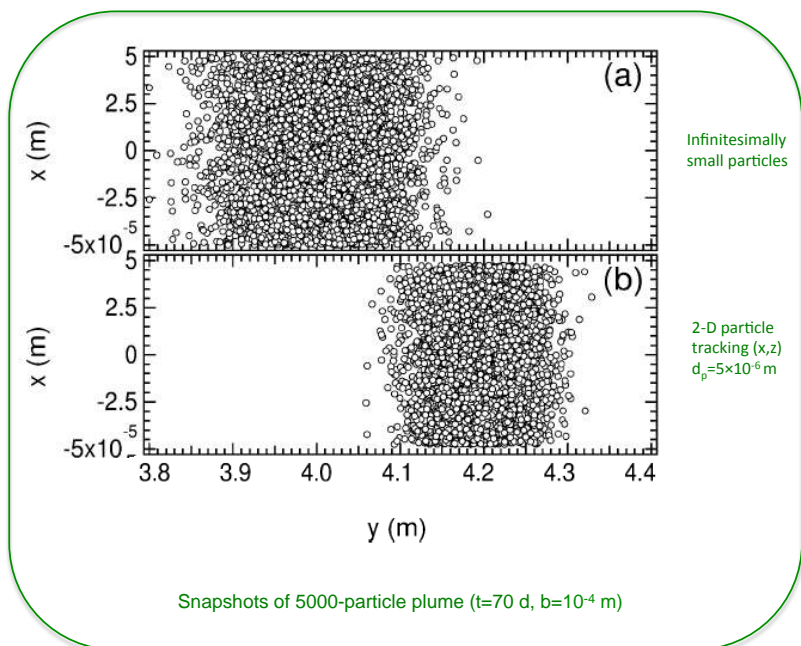


$$U_{\text{eff}} = \frac{2}{3} U_{\text{max}} \left[ 1 + \frac{d_p}{b} - \frac{1}{2} \left( \frac{d_p}{b} \right)^2 \right]$$

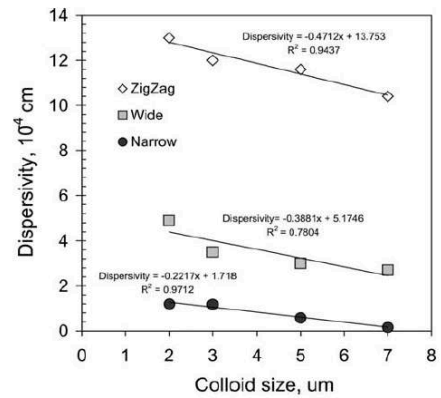
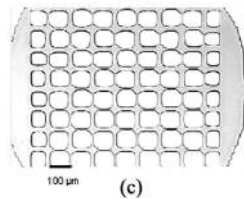
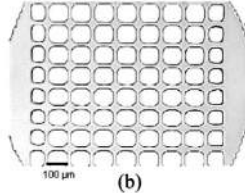
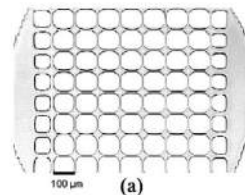
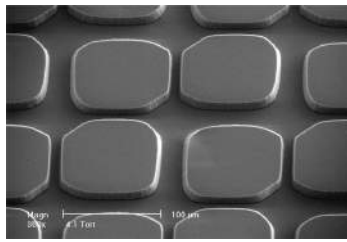
$$D_{\text{eff}} = D + \frac{2}{945} \frac{U_{\text{max}}^2 b^2}{D} \left( 1 - \frac{d_p}{b} \right)^6$$

$$D_{\text{Taylor}} = D + \frac{2}{945} \frac{U_{\text{max}}^2 b^2}{D}$$

$$D = \frac{kT}{3\pi\eta d_p}$$



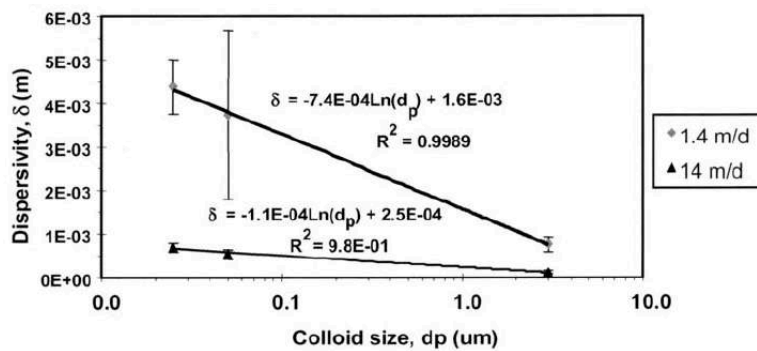
## Early work on particle size-dependent dispersivity (Micromodel)



Mass recovered:  $M_r = 100\%$

Reference: Auset and Keller, WRR, 2004.

## Early work on particle size-dependent dispersivity (Column study)



Mass recovered:  $M_r = 28.8$  to  $41.0\%$

Reference: Keller, Sirivithayapakorn, and Chrysikopoulos, WRR, 2004.

**Question:** Should dispersivity decrease or increase with colloid particle size?

## Another look at particle size-dependent dispersivity

### Materials and methods

- Columns:** diameter = 2.5 cm  
length = 15 & 30 cm  
packed with glass beads ( $d_c=2$  mm)  
placed horizontally to minimize gravity effects
- Colloids:** fluorescent polystyrene microspheres  
 $d_p = 28, 300, 600, 1000, 1750, 2100, 3000, 5000$  and 5500 nm  
fluorescence spectrophotometry
- Tracer:** bromide in the form of NaBr ( $10^{-5}$  M)  
ion chromatography
- Source:** “instantaneous” pulse
- $d_p/d_c$ :** <0.00275  
below the straining and wedging threshold of  
>0.004 (Johnson et al., 2010) or  
>0.003 (Bradford and Bettahar, 2006)

Transport experiments were performed under unfavorable colloid attachment conditions ( $\text{pH}=7, I_s=0.1$  mM).

# Mathematical Model

## Governing transport equation

(Sim and Chrysikopoulos, WRR, 1998)

$$\frac{\partial C(t,x)}{\partial t} + \frac{\rho_b}{\theta} \frac{\partial C^*(t,x)}{\partial t} = D_L \frac{\partial^2 C(t,x)}{\partial x^2} - U \frac{\partial C(t,x)}{\partial x} - \lambda C(t,x) - \lambda^* \frac{\rho_b}{\theta} C^*(t,x)$$

Colloid attachment onto the solid matrix

$$\frac{\rho_b}{\theta} \frac{\partial C^*(t,x)}{\partial t} = k_c C(t,x) - k_r \frac{\rho_b}{\theta} C^*(t,x) - \lambda^* \frac{\rho_b}{\theta} C^*(t,x)$$

Assuming that  $C^*(0,x)=0$

$$C^*(t,x) = \frac{k_c \theta}{\rho_b} \int_0^t C(\tau,x) \exp\left[-\left(k_r \frac{\theta}{\rho_b} + \lambda^*\right)(t-\tau)\right] d\tau$$

Initial and boundary conditions

$$C(0,x) = 0$$

$$-D_L \frac{\partial C(t,0)}{\partial x} + UC(t,0) = M_\delta \delta(t)$$

$$M_\delta = \frac{M_{in}}{A_c \theta}$$

$$\frac{\partial C(t,\infty)}{\partial x} = 0$$

## Analytical solution

(Thomas and Chrysikopoulos, JoCIS, 2007)

$$\begin{aligned} C(t,x) = & \frac{M_\delta}{D^{1/2}} \exp\left[\frac{Ux}{2D_L} - Ht\right] \left\{ \frac{1}{(\pi t)^{1/2}} \exp\left[\frac{-x^2}{4D_L t} + \left(H - A - \frac{U^2}{4D_L}\right)t\right] \right. \\ & - \frac{U}{2D_L^{1/2}} \exp\left[\frac{Ux}{2D_L} + (H-A)t\right] \operatorname{erfc}\left[\frac{x}{2(D_L t)^{1/2}} + \frac{U}{2}\left(\frac{t}{D_L}\right)^{1/2}\right] \\ & + \int_0^t \frac{B\zeta}{\{B\zeta(t-\zeta)\}^{1/2}} I_1\left[2(B\zeta(t-\zeta))^{1/2}\right] \left\{ \frac{1}{(\pi\zeta)^{1/2}} \exp\left[\frac{-x^2}{4D_L \zeta} + \left(H - A - \frac{U^2}{4D_L}\right)\zeta\right] \right. \\ & \left. \left. - \frac{U}{2D_L^{1/2}} \exp\left[\frac{Ux}{2D_L} + (H-A)\zeta\right] \operatorname{erfc}\left[\frac{x}{2(D_L \zeta)^{1/2}} + \frac{U}{2}\left(\frac{\zeta}{D_L}\right)^{1/2}\right] \right\} d\zeta \right\} \end{aligned}$$

$$A = k_c + \lambda, \quad B = \frac{k_c k_r \theta}{\rho_b}, \quad H = \frac{k_c \theta}{\rho_b} = \lambda^*$$

$I_1$  = Modified Bessel function (first-kind, order-one)

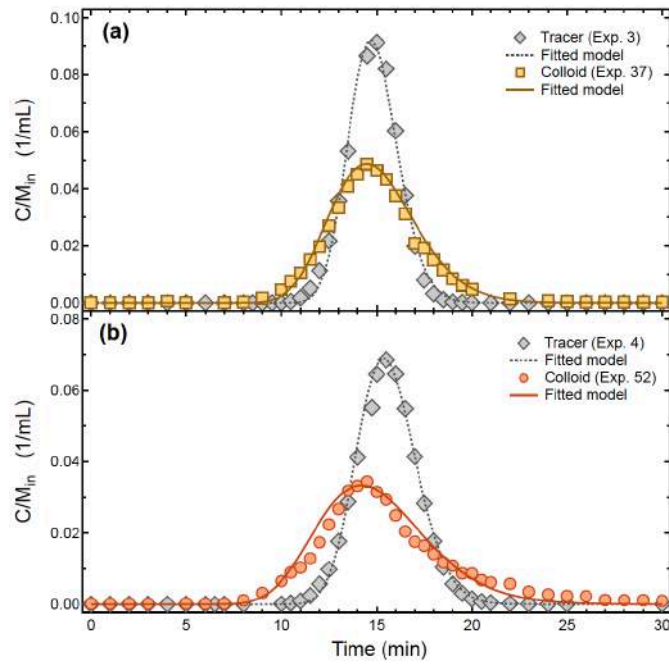


**Figure A1.** Early breakthrough

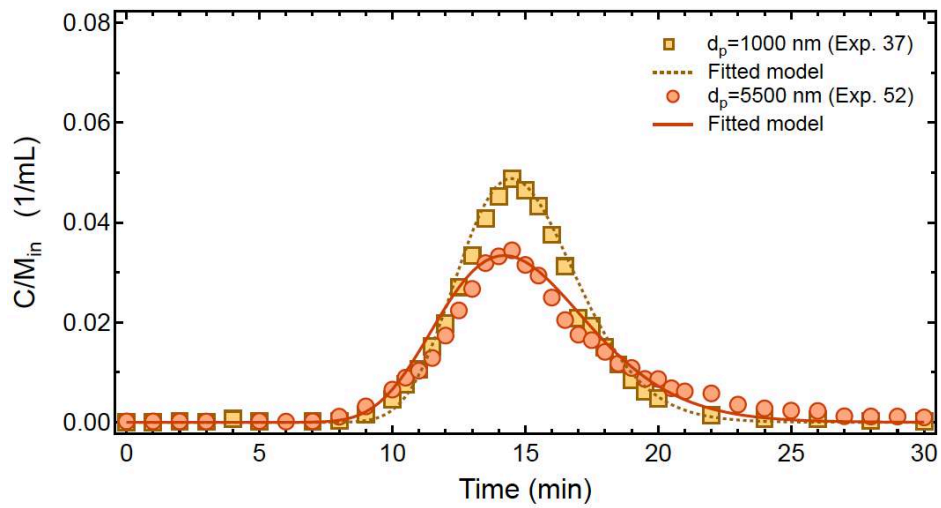


**Figure A2.** Breakthrough curves for two different colloids

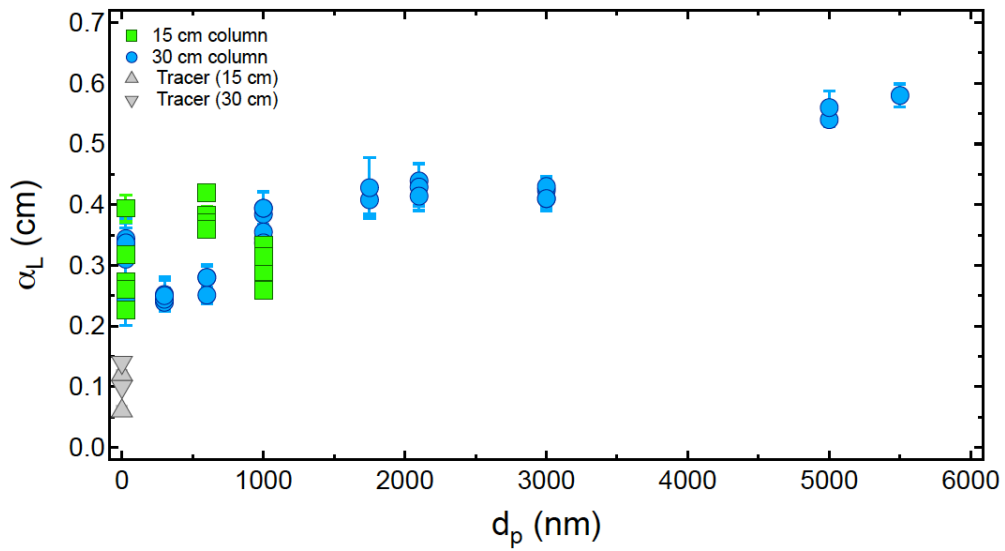


**Figure A3.** Longitudinal dispersivity as a function of colloid diameter.

Hypothesis that the population regression is linear: Accepted  
 F test-Hypothesis that the slope=0: Rejected

(Chrysikopoulos and Katzourakis, WRR, 2015)

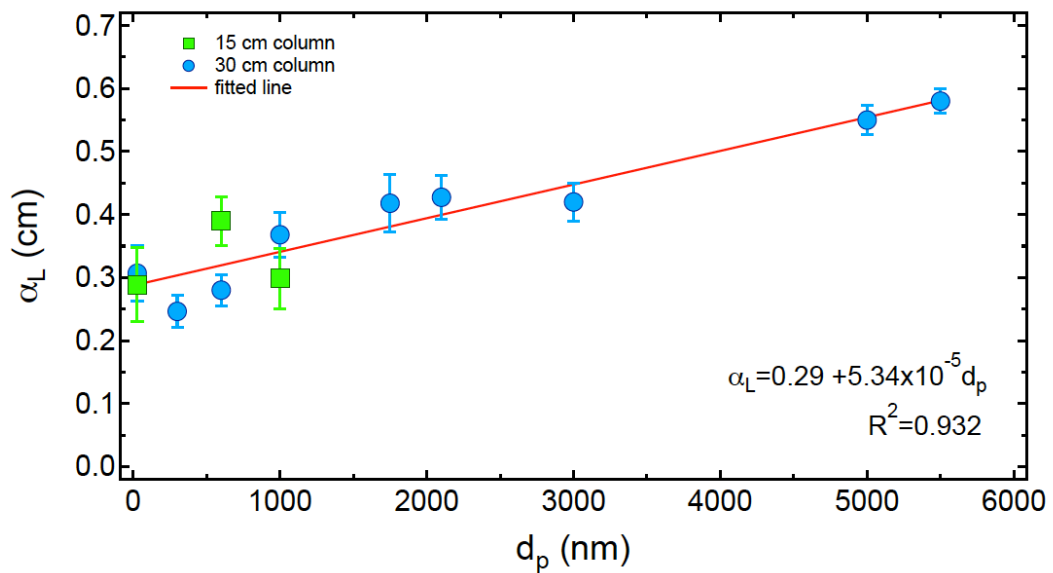


**Figure A4.** Longitudinal dispersivity (averaged) as a function of colloid diameter.

(Chrysikopoulos and Katzourakis, WRR, 2015)

## Scaling of $D_L$ with Peclet number

(Delgado, 2007)

$$\frac{D_L}{\mathcal{D}_e} = \frac{Pe_m}{6} \left[ \ln \left( \frac{3\tau}{2} Pe_m \right) - \frac{1}{4} \right], \quad Pe_m \gg 1$$

$$Pe_m = \frac{Ud_c}{\mathcal{D}_e} \quad [-]$$

$$250 < Pe_m < 10^5$$

Molecular diffusion is negligible.

Mechanical dispersion is the governing dispersion process.

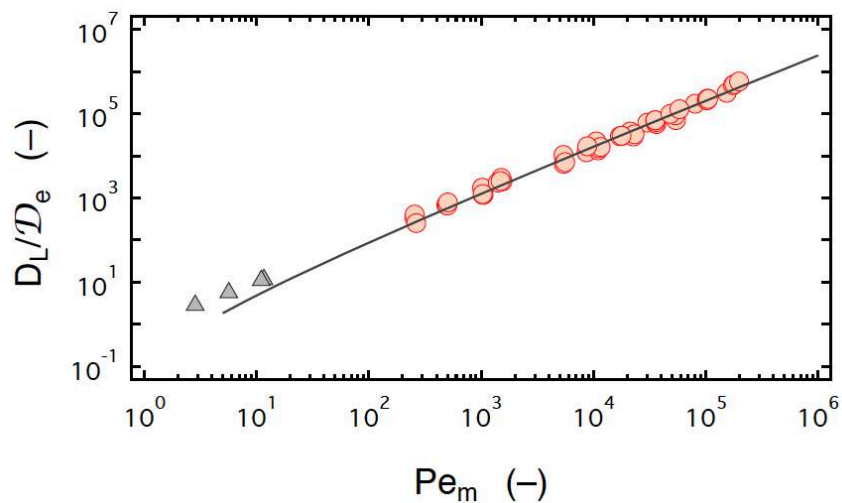


**Figure A10.** Scaling of the longitudinal hydrodynamic dispersion coefficients (circles for colloids, and triangles for tracer) with Péclet number.

## Mass Recovery

$$M_r(L) = \frac{m_0(L)}{M_0/U}$$

$$m_0(L) = \int_0^{\infty} C(L,t) dt \quad \left[ \frac{tM}{L^3} \right]$$

Zeroth absolute temporal moment

(Quantifies the total mass in the concentration distribution curve)

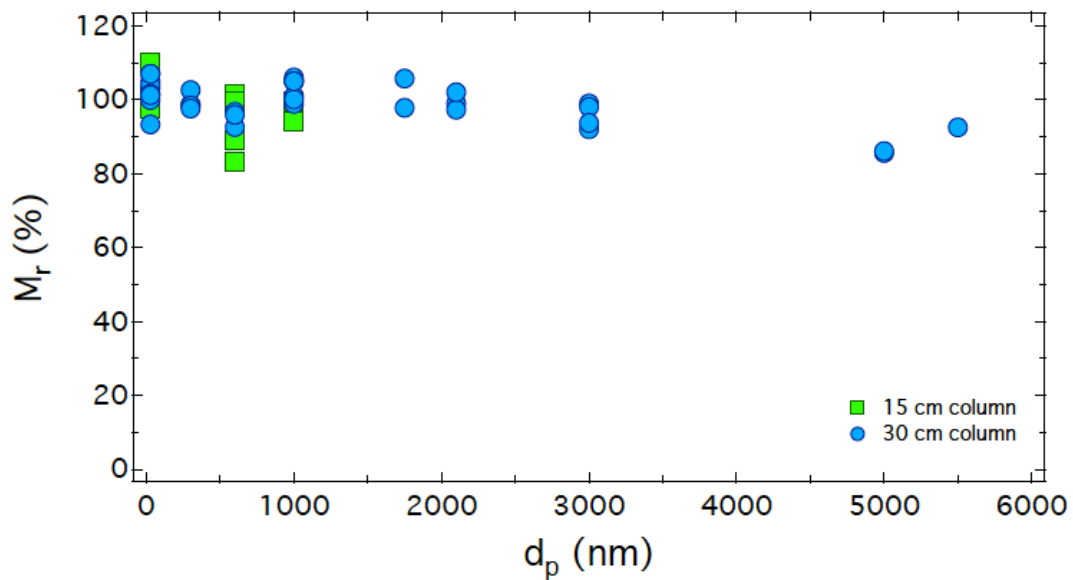


**Figure A8.** Mass recovery as a function of particle size

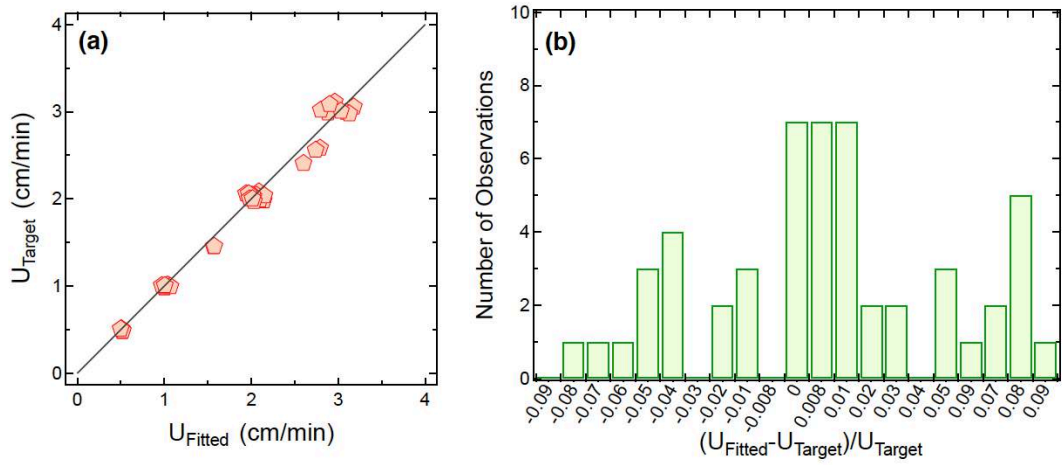


**Figure A9.** Comparison between the target interstitial velocities (based on Q) and fitted colloid particle velocities .

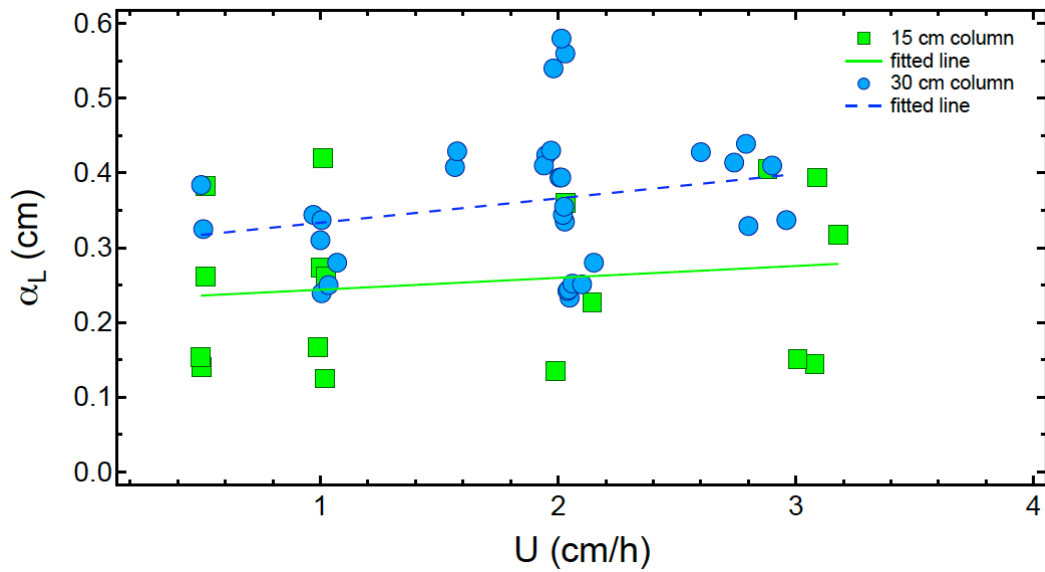


**Figure A6.** Longitudinal dispersivity as a function of interstitial velocity

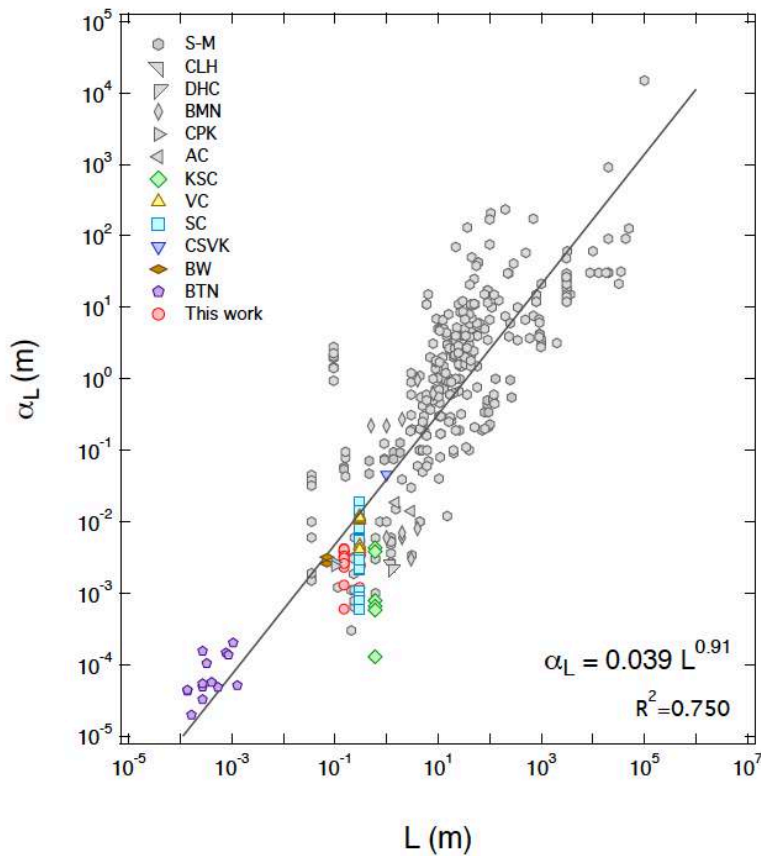


**Figure A7.** Compilation of 432 longitudinal dispersivities as a function of length scale. Molecular sized solutes are represented by gray symbols, and colloids/biocolloids by various colored symbols. The solid line is a standard linear regression line.

**References:**

- S-M [Schulze-Makuch, 2005]
- CLH [Chrysikopoulos et al., 2000]
- DHC [Dela Barre et al., 2002]
- BMN [Baumann et al., 2002]
- CPK [Chrysikopoulos et al., 2011]
- AC [Anders and Chrysikopoulos, 2005]
- KSC [Keller et al., 2004]
- VC [Vasiliadou & Chrysikopoulos, 2011]
- SC [Syngouna & Chrysikopoulos, 2011]
- CSVK [Chrysikopoulos et al., 2012]
- BW [Bauman and Werth, 2004]
- BTN [Baumann et al., 2010]

**Explanation**

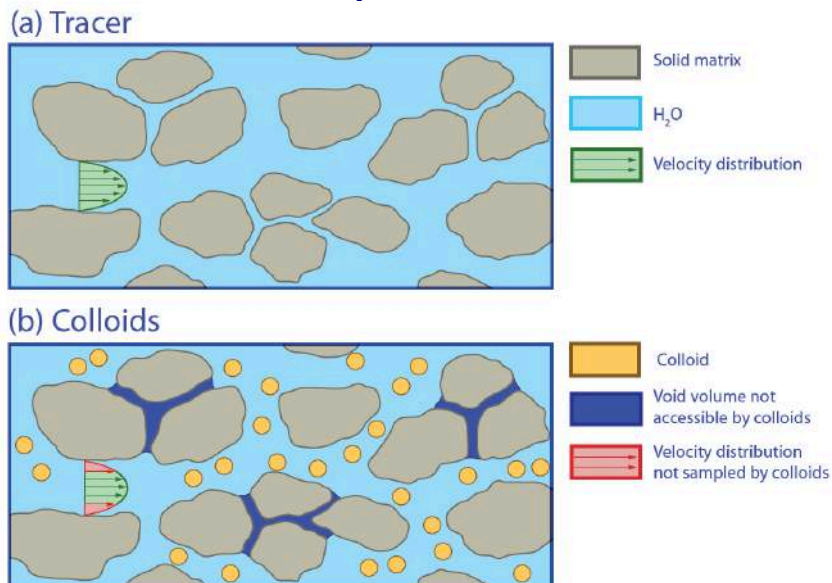


**Figure A5.** Schematic illustration of: (a) conservative solute and (b) colloid transport in water saturated porous media.

The tracer can sample the entire velocity spectrum within the parabolic profile (green region). Colloids do not sample the truncated portion of the parabolic velocity profile (red region). Also, colloids do not enter pore spaces with opening smaller than  $d_p$ , which essentially leads to reduction of effective porosity.

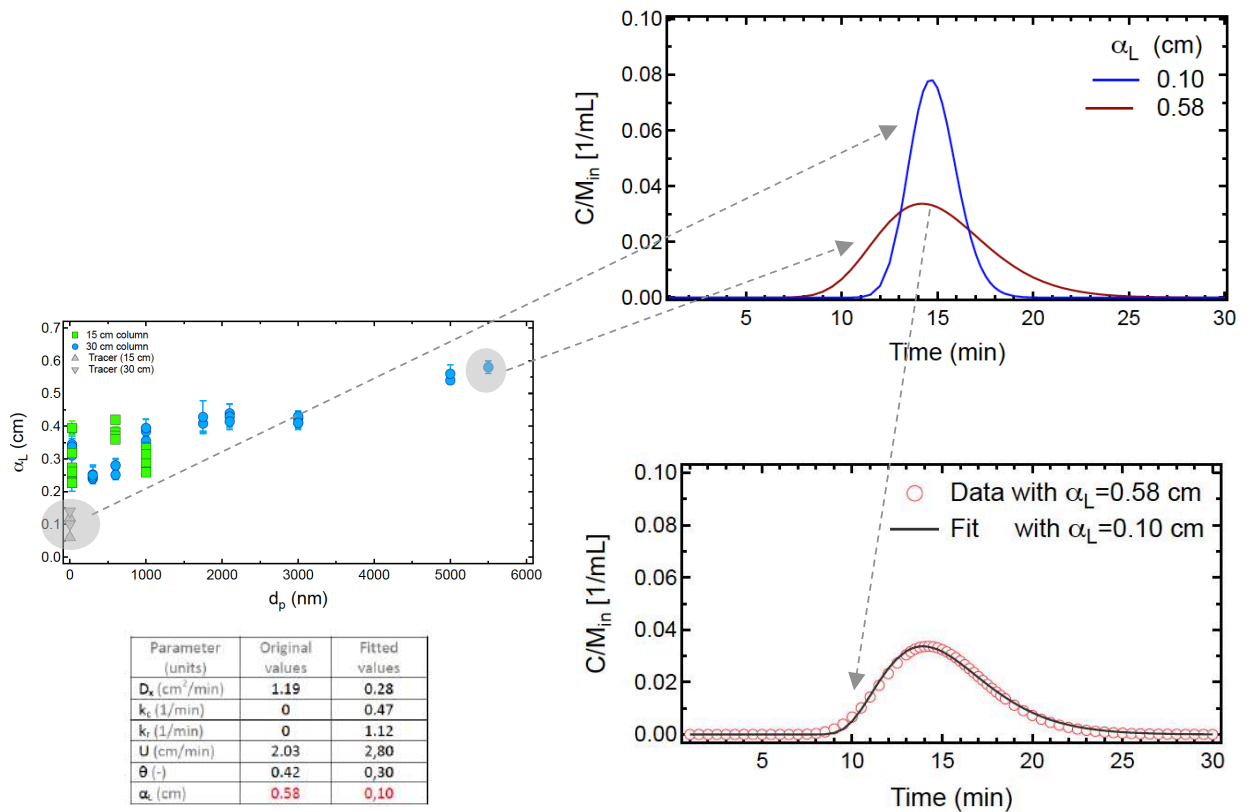
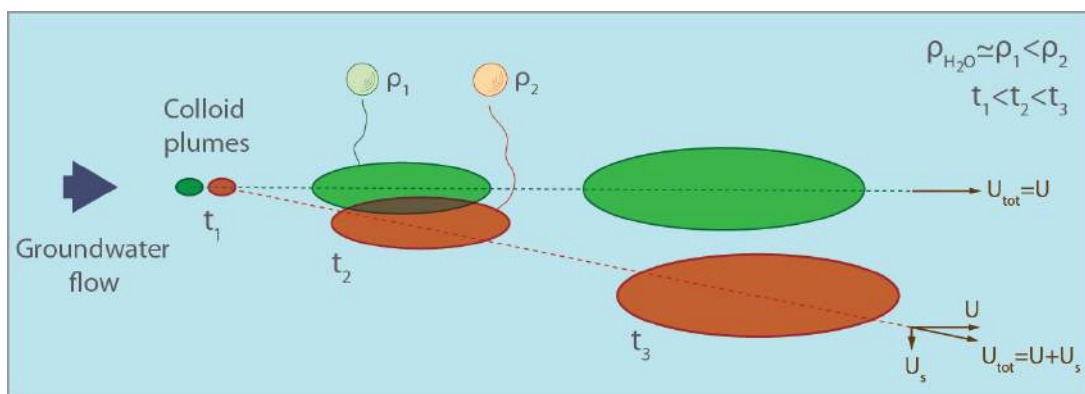
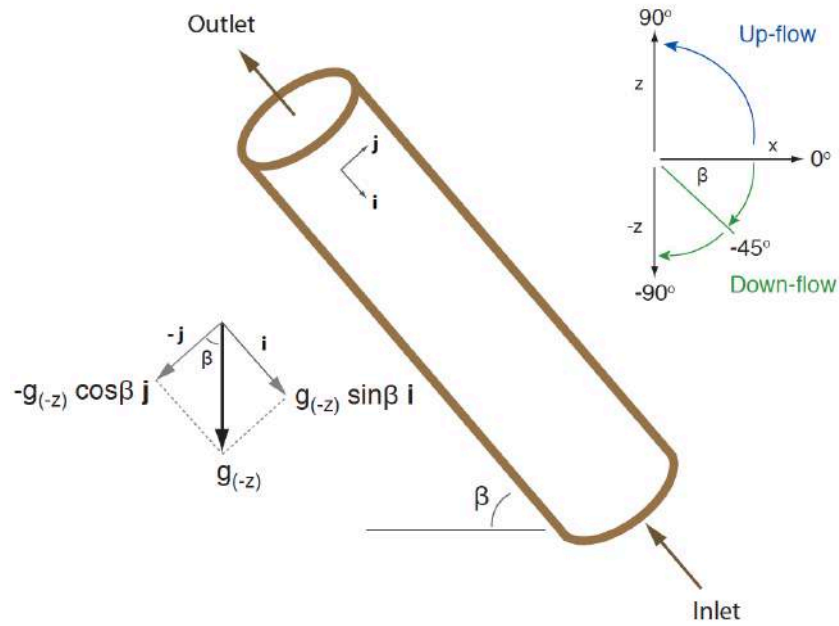


Figure A9. How “garbage” results are often produced.

## Part B: Gravity effects





**Figure B1.** Schematic illustration of a packed column with up-flow velocity having orientation ( $-i$ ) with respect to gravity. The gravity vector components are:  
 $g_{(i)} = g_{(-z)} \sin \beta$   $i$ , and  $g_{(-j)} = -g_{(-z)} \cos \beta$   $j$ .

## “restricted” particle settling velocity

$$U_s = -f_s \frac{(\rho_p - \rho_w) d_p^2}{18\mu_w} g_{(i)}$$

$$g_{(i)} = g_{(-z)} \sin \beta$$

$f_s$  [-] = correction factor accounting for particle settling in granular porous media (Wan et al., 1995)

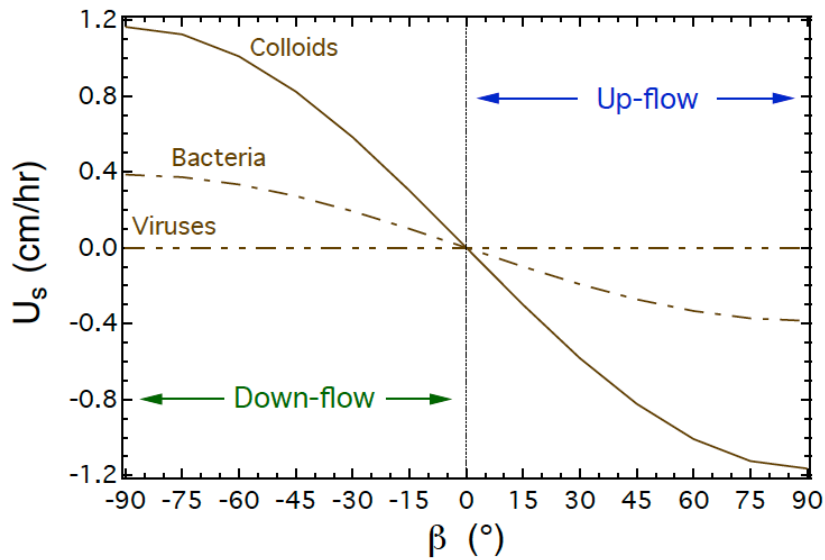


**Figure B2.** Restricted particle settling velocity as a function of column orientation and flow direction for colloids (clay:  $d_p=2 \mu\text{m}$ ,  $\rho_p=2.65 \text{ g/cm}^3$ ), bacteria (*P. putida*:  $d_p=2.2 \mu\text{m}$ ,  $\rho_p=1.45 \text{ g/cm}^3$ ), and viruses (MS2:  $d_p=25 \text{ nm}$ ,  $\rho_p=1.42 \text{ g/cm}^3$ ).

## Mathematical Model

### Governing transport equation

$$\frac{\partial C(t,x)}{\partial t} + \frac{\rho_b}{\theta} \frac{\partial C^*(t,x)}{\partial t} = D \frac{\partial^2 C(t,x)}{\partial x^2} - U_{\text{tot}} \frac{\partial C(t,x)}{\partial x} - \lambda C(t,x) - \lambda^* \frac{\rho_b}{\theta} C^*(t,x)$$

$$U_{\text{tot}} = U + U_s$$

### Colloid attachment onto the solid matrix

(Sim and Chrysikopoulos, TiPM, 1998)

$$\frac{\rho_b}{\theta} \frac{\partial C^*(t,x)}{\partial t} = k_c C(t,x) - k_r \frac{\rho_b}{\theta} C^*(t,x) - \lambda^* \frac{\rho_b}{\theta} C^*(t,x)$$

### Initial and boundary conditions

$$C(0,x) = 0$$

$$-D \frac{\partial C(t,0)}{\partial x} + U_{\text{tot}} C(t,0) = \begin{cases} U_{\text{tot}} C_0 & 0 < t \leq t_p \\ 0 & t > t_p \end{cases}$$

$$\frac{\partial C(t,\infty)}{\partial x} = 0$$

# Analytical solution

(Sim and Chrysikopoulos, WRR, 1996)

$$C(t, x) = \begin{cases} \Omega(t, x) & 0 < t \leq t_p \\ \Omega(t, x) - \Omega(t - t_p, x) & t > t_p \end{cases}$$

$$\begin{aligned} \Omega(t, x) = & \frac{C_0 U_{tot}}{D^{3/2}} \exp\left[\frac{U_{tot} x}{2D}\right] \left\{ \int_0^t \int_0^\tau H e^{-H\tau} J_0 \left[ 2(B\xi(\tau - \xi))^{1/2} \right] \right. \\ & \cdot \left. \left\{ \frac{1}{(\pi\xi)^{1/2}} \exp\left[ \frac{-x^2}{4D\xi} + \left( H - A - \frac{U_{tot}^2}{4D} \right) \xi \right] \right. \right. \\ & - \frac{U_{tot}}{2D^{1/2}} \exp\left[ \frac{U_{tot} x}{2D} + (H - A)\xi \right] \\ & \cdot \left. \left. \operatorname{erfc} \left[ \frac{x}{2(D\xi)^{1/2}} + \frac{U_{tot}}{2} \left( \frac{\xi}{D} \right)^{1/2} \right] \right\} d\xi d\tau \right. \\ & + e^{-Ht} \int_0^t J_0 \left[ 2(B\xi(t - \xi))^{1/2} \right] \\ & \cdot \left. \left\{ \frac{1}{(\pi\xi)^{1/2}} \exp\left[ \frac{-x^2}{4D\xi} + \left( H - A - \frac{U_{tot}^2}{4D} \right) \xi \right] \right. \right. \\ & - \frac{U_{tot}}{2D^{1/2}} \exp\left[ \frac{U_{tot} x}{2D} + (H - A)\xi \right] \\ & \cdot \left. \left. \operatorname{erfc} \left[ \frac{x}{2(D\xi)^{1/2}} + \frac{U_{tot}}{2} \left( \frac{\xi}{D} \right)^{1/2} \right] \right\} d\xi \right\}. \end{aligned}$$

$$A = k_c + \lambda,$$

$$B = k_c k_f \theta / \rho,$$

$$H = (k_c \theta / \rho) + \lambda^*,$$

$J_0$  = Bessel function (first-kind of zeroth-order)

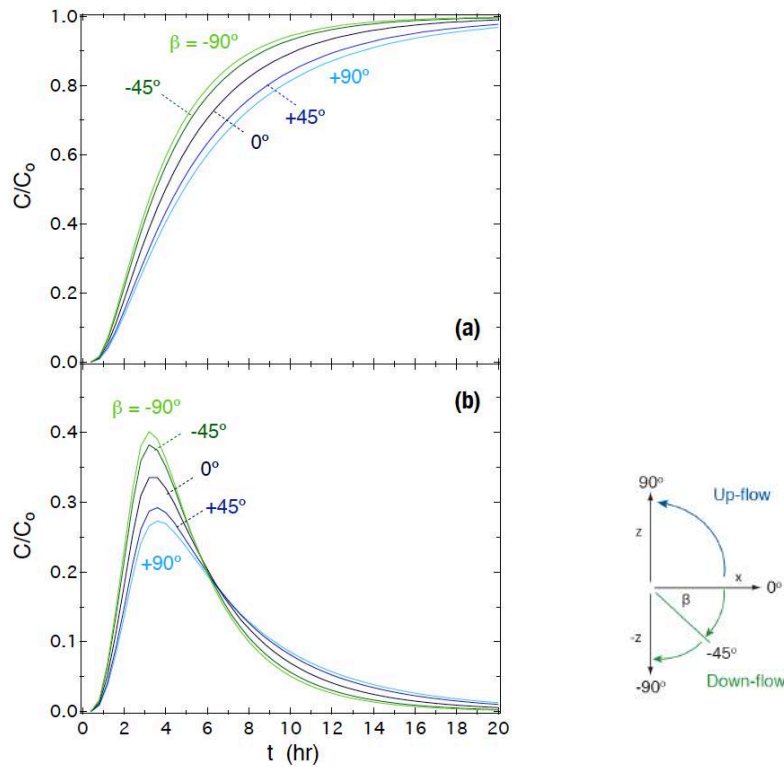


**Figure B3.** Simulations of normalized colloid breakthrough curves for packed columns with various orientations and flow directions under: (a) continuous, and (b) broad pulse inlet boundary conditions.

# Materials & methods

**Columns:** diameter = 2.5 cm  
length = 30 cm  
packed with glass beads ( $d_c = 2$  mm)  
columns were placed horizontally ( $0^\circ$ ),  
vertically ( $90^\circ$ ),  
inclined ( $45^\circ$ ).

**Clays:** kaolinite (KGa-1b), specific surface area of  $10.1$  m<sup>2</sup>/g,  
 $d_p = 843 \pm 126$  nm  
montmorillonite (STx-1b), specific surface area of  $82.9$  m<sup>2</sup>/g,  
 $d_p = 1187 \pm 381$  nm  
 $C_o = 10^7$  to  $10^{13}$  particles/mL  
detection by UV-vis spectrophotometer

**Tracer:** bromide in the form of NaBr ( $10^{-5}$  M)  
ion chromatography

Unfavorable to deposition transport conditions ( $\text{pH}=7$ ,  $I_s=0.1\text{mM}$ ).  
Experimental data fitted with ColloidFit.

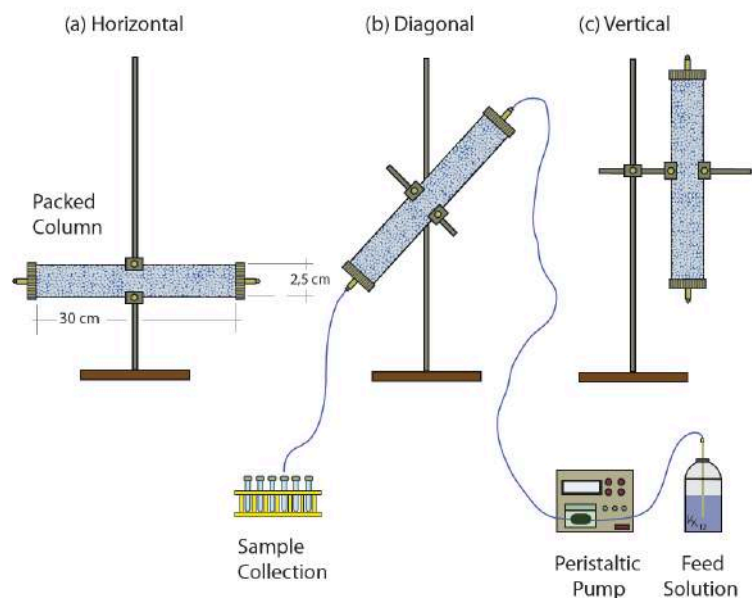
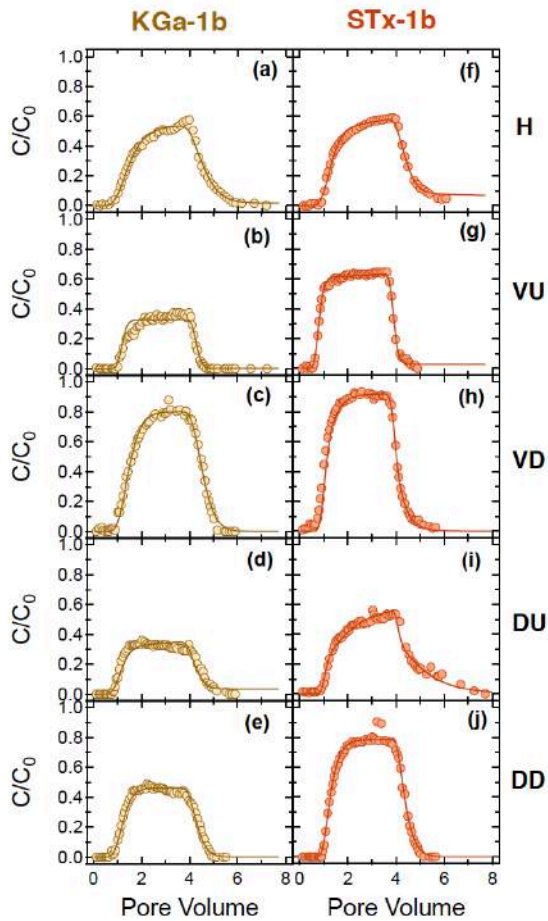


**Figure B4.** Experimental setup showing the various column arrangements:  
(a) horizontal, (b) diagonal, and (c) vertical.



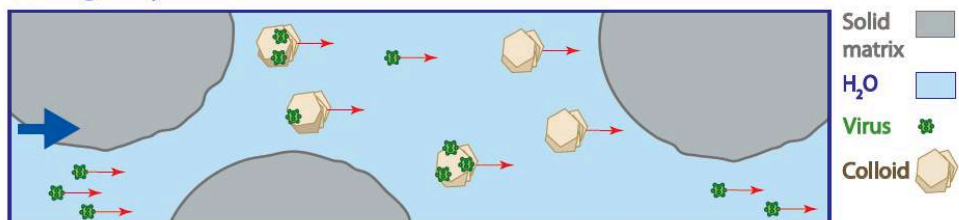
kaolinite: KGa-1b  
montmorillonite: STx-1b

H: horizontal  
VU: vertical up-flow  
VD: vertical down-flow  
DU: diagonal up-flow  
DD: diagonal down-flow

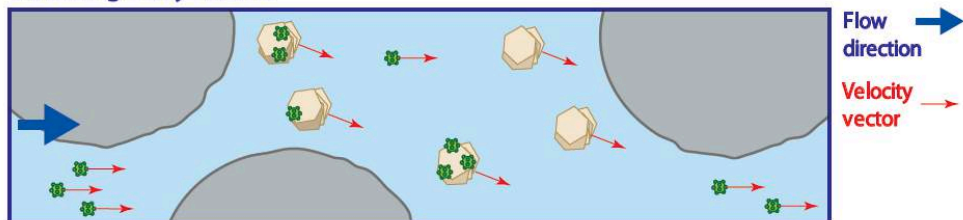
**Figure B5.** Experimental data (symbols) and fitted model simulations (curves)  
(Chrysikopoulos and Syngouna, ES&T, 2014)

## Part C: Clay & virus cotransport

(a) no gravity effects



(b) with gravity effects



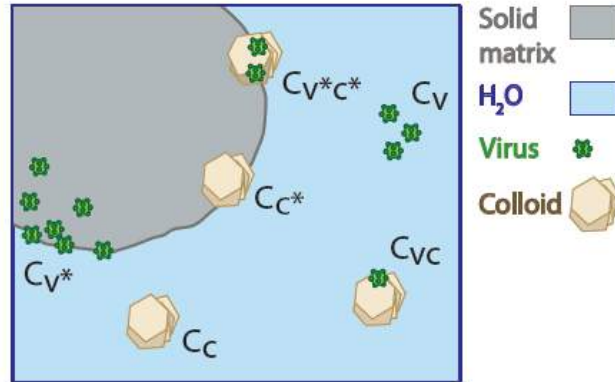


**Figure C2.** Schematic illustration of the various concentrations accounted for in the cotransport numerical model

### Three-dimensional cotransport mathematical model – (Transport of dense colloids)

#### Governing transport equation

(Katzourakis and Chrysikopoulos, AWR, 2014 & JoCH 2015)

$$\frac{\partial C_c}{\partial t} + \frac{\rho_b}{\theta} \frac{\partial C_{c^*}}{\partial t} - D_{xc} \frac{\partial^2 C_c}{\partial x^2} - D_{yc} \frac{\partial^2 C_c}{\partial y^2} - D_{zc} \frac{\partial^2 C_c}{\partial z^2} + (U_x + U_{cs(\pm)}) \frac{\partial C_c}{\partial x} + U_{cs(-k)} \frac{\partial C_c}{\partial z} = F_c$$

$$U_{cs(\pm)} = f_s \frac{(\rho_p - \rho_w) d_p^2}{18 \mu_w} g_{(\pm)} \quad g_{(\pm)} = g \cos \beta$$

$$U_{cs(-k)} = f_s \frac{(\rho_p - \rho_w) d_p^2}{18 \mu_w} g_{(-k)} \quad g_{(-k)} = -g \sin \beta$$

#### Colloid attachment onto the solid matrix

(Sim and Chrysikopoulos, 1998; Compere et al., 2001)

$$C_{c^*} = C_{c^*(r)} + C_{c^*(i)} \Rightarrow \frac{\rho_b}{\theta} \frac{\partial C_{c^*}}{\partial t} = \frac{\rho_b}{\theta} \left[ \frac{\partial C_{c^*(r)}}{\partial t} + \frac{\partial C_{c^*(i)}}{\partial t} \right]$$

$$\frac{\rho_b}{\theta} \frac{\partial C_{c^*(r)}}{\partial t} = r_{c-c^*(i)} C_c - r_{c^*(i)-c} \frac{\rho_b}{\theta} C_{c^*(r)}$$

$$\frac{\rho_b}{\theta} \frac{\partial C_{c^*(i)}}{\partial t} = r_{c-c^*(i)} C_c$$

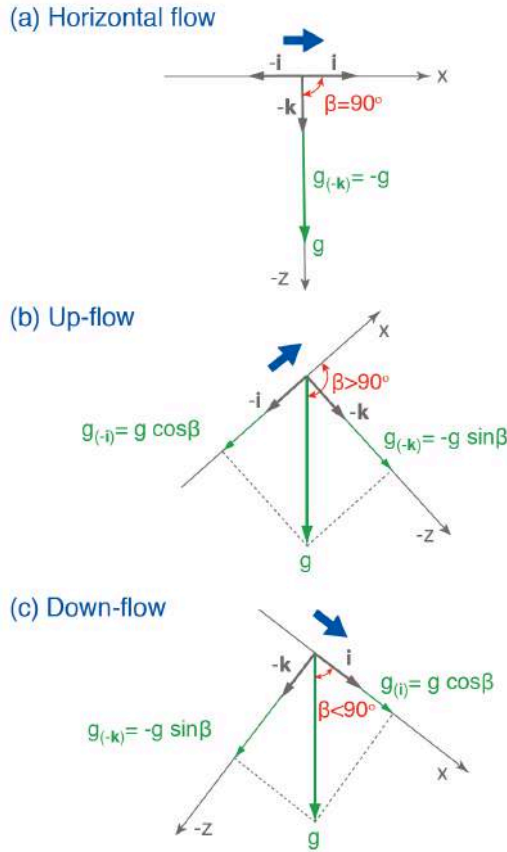


**Figure C1.** Schematic illustration of the gravity vector components for: (a) horizontal flow, (b) up-flow, and (c) down-flow conditions. The angle  $\beta$  ( $0^\circ \leq \beta \leq 180^\circ$ ) is between the main flow direction (x-direction) and the direction of gravity.

### Three-dimensional cotransport mathematical model – (Transport of viruses)

#### Governing transport equation

(Abdel-Salam and Chrysikopoulos, 1995; Vasiliadou and Chrysikopoulos, 2011; Katzourakis and Chrysikopoulos, 2014)

$$\begin{aligned} \frac{\partial}{\partial t} (C_v + \frac{\rho_b}{\theta} C_{v^*} + C_c C_{vc} + \frac{\rho_b}{\theta} C_c C_{v^*c^*}) &= D_{xv} \frac{\partial^2 C_v}{\partial x^2} + D_{xvc} \frac{\partial^2}{\partial x^2} (C_c C_{vc}) + D_{yv} \frac{\partial^2 C_v}{\partial y^2} \\ &+ D_{yvc} \frac{\partial^2}{\partial y^2} (C_c C_{vc}) + D_{zv} \frac{\partial^2 C_v}{\partial z^2} + D_{zvc} \frac{\partial^2}{\partial z^2} (C_c C_{vc}) \\ &- (U_x + U_{vs(z)}) \frac{\partial}{\partial x} (C_v + C_c C_{vc}) - U_{vs(-k)} \frac{\partial}{\partial z} (C_v) - U_{vcs(-k)} \frac{\partial}{\partial z} (C_c C_{vc}) \\ &- \lambda_v C_v - \lambda_{vc} C_v C_{vc} - \lambda_{v^*} \frac{\rho_b}{\theta} C_{v^*} - \lambda_{v^*c^*} \frac{\rho_b}{\theta} C_c C_{v^*c^*} + F_v(t, x, y, z) \end{aligned}$$

#### Accumulation terms

(Sim and Chrysikopoulos, 1998; Bekhit et al., 2009; Katzourakis and Chrysikopoulos, 2014)

$$\begin{aligned} \frac{\rho_b}{\theta} \frac{\partial C_{v^*}}{\partial t} &= r_{v-v^*} C_v - r_{v^*-v} \frac{\rho_b}{\theta} C_{v^*} - \lambda_{v^*} \frac{\rho_b}{\theta} C_{v^*} \\ \frac{\partial}{\partial t} (C_c C_{vc}) &= r_{v-vc} (C_c)^2 C_v - r_{vc-v} (C_c C_{vc}) + \frac{\rho_b}{\theta} r_{v^*c^*-vc} (C_c C_{v^*c^*}) - r_{vc-v^*c^*} (C_c C_{vc}) - \lambda_{vc} C_c C_{vc} \\ \frac{\rho_b}{\theta} \frac{\partial}{\partial t} (C_c C_{v^*c^*}) &= \frac{\rho_b}{\theta} r_{v-v^*c^*} (C_c)^2 C_v - \frac{\rho_b}{\theta} r_{v^*c^*-v} (C_c C_{v^*c^*}) + r_{vc-v^*c^*} (C_c C_{vc}) - \frac{\rho_b}{\theta} r_{v^*c^*-vc} (C_c C_{v^*c^*}) - \lambda_{v^*c^*} \frac{\rho_b}{\theta} C_c C_{v^*c^*} \end{aligned}$$

#### Source configurations

$$F_v(t, x, y, z) = 1 \delta(x-40) \delta(y-15) \delta(z-15) \frac{\text{pfu}}{\text{mL} \cdot \text{hr}}$$

$$F_c(t, x, y, z) = \begin{cases} 100 \frac{\text{mg}}{\text{mL} \cdot \text{hr}} & \frac{(x-6)^2}{0.4^2} + \frac{(y-15)^2}{0.3^2} + \frac{(z-15)^2}{0.3^2} \leq 1 \\ 0 & \text{otherwise} \end{cases}$$

#### Initial and boundary conditions

$$C_i(0, x, y, z) = 0$$

$$\frac{\partial^2 C_i(t, 0, y, z)}{\partial x^2} = \frac{\partial^2 C_i(t, L_x, y, z)}{\partial x^2} = 0$$

$$\frac{\partial C_i(t, x, 0, z)}{\partial y} = \frac{\partial C_i(t, x, L_y, z)}{\partial y} = \frac{\partial C_i(t, x, y, 0)}{\partial z} = \frac{\partial C_i(t, x, y, L_z)}{\partial z} = 0$$

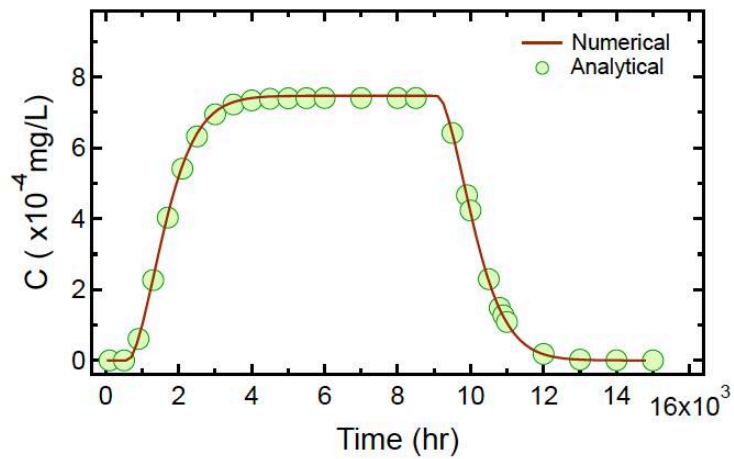


**Figure C3.** Comparison of analytical (circles) and numerical solutions (solid curve). Here the duration period of the source is  $t_p = 8500$  hr, the concentrations are evaluated at  $x=60$  m,  $y=15$  m and  $z=15$  m.

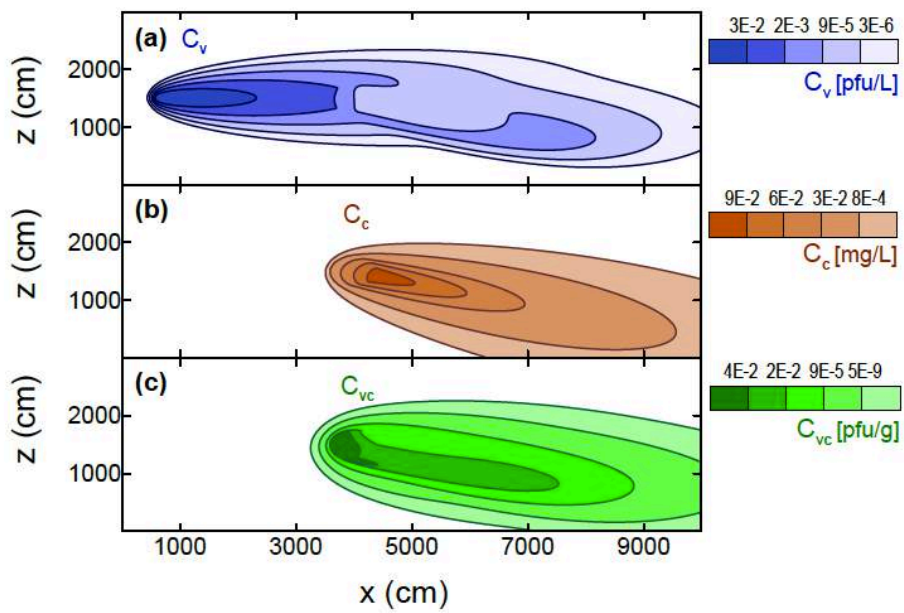


**Figure C4.** Concentration contour plots on the x-z plane for: (a) viruses, (b) colloids, and (c) virus-colloid particles during virus and colloid cotransport, accounting for gravitational effects. Here  $t=6900$  hr, and  $y=15$  m.

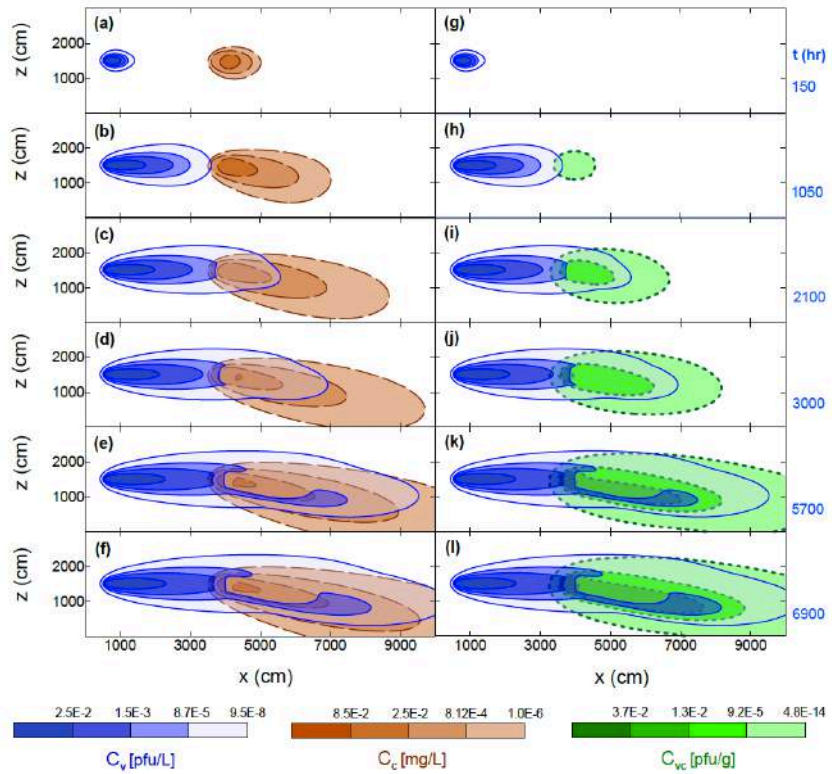


**Figure C5.** Contour plots on the  $x$ - $z$  plane for: (a-f) viruses (solid curves) and colloid particles (dashed curves), and (g-l) viruses (solid curves) and virus-colloid particles (dotted curves) during virus and colloid cotransport in the presence of gravitational effects.

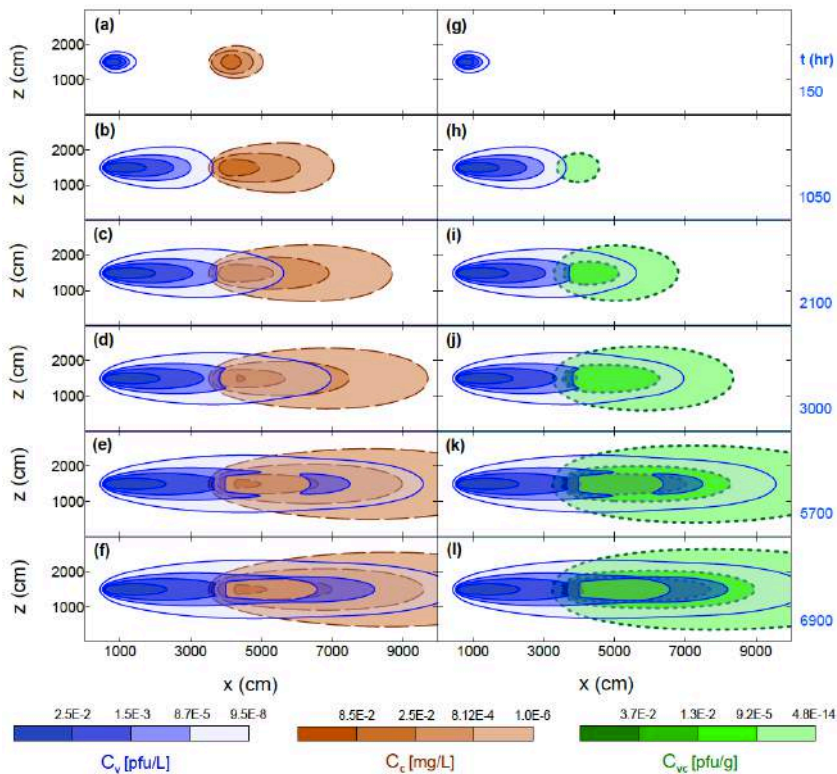


**Figure C6.** Contour plots on the  $x$ - $z$  plane for: (a-f) viruses (solid curves) and colloid particles (dashed curves), and (g-l) viruses (solid curves) and virus-colloid particles (dotted curves) during virus and colloid cotransport in the absence of gravitational effects.

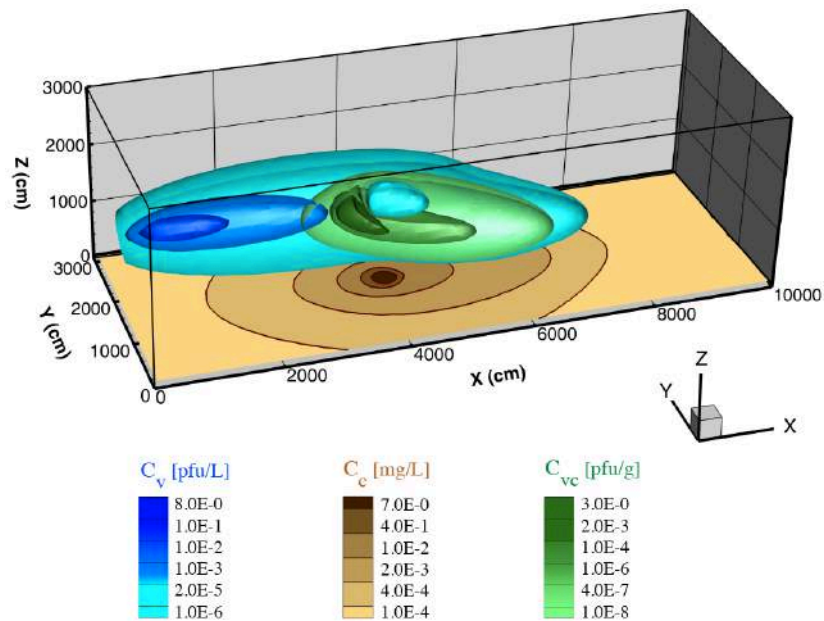


**Figure C7.** Isosurface three-dimensional concentrations plots for viruses (blue surfaces) and virus-colloid particles (green surfaces), along with a projected contour plot on the x-y plane at  $z=15$  m for colloid particles (brown contour). Here  $t=13000$  hr.

## Summary

### A: Size-dependent dispersivity

- Colloid dispersivity is not only a function of scale, but also a function of colloid diameter and interstitial velocity.
- Contrary to earlier results, colloid dispersivity increases with increasing colloid diameter and interstitial velocity.
- Fitted dispersion coefficients based on tracer data should not be used to analyze colloid data.

### B: Gravity effects

- Flow direction influences colloid transport in porous media.

### C: Cotransport with gravity effects

- The presence of dense colloids influence contaminant transport in porous media.
- Dense colloids can increase the vertical migration of viruses.

**Thank you**  
**for your attention**